

Voltage Transfer Ratio Improvement of an Indirect Matrix Converter by Single Pulse Modulation

Goh Teck Chiang

Student Member, IEEE

Nagaoka University of Technology
1603-1 Kamitomioka,
Nagaoka Niigata, 940-2188, Japan
tcgoh@stn.nagaokaut.ac.jp

Jun-ichi Itoh

Member, IEEE

Nagaoka University of Technology
1603-1 Kamitomioka,
Nagaoka Niigata, 940-2188, Japan
itoh@vos.nagaokaut.ac.jp

Abstract—This paper proposes two over modulation strategies for the Indirect Matrix Converter (IMC). These strategies aim to improve the output-input voltage transfer ratio of the converter and also maintain high efficiency. This paper will discuss the control method of the two modulations and also compare the total losses of the converter. The control method uses a triangular carrier comparison method which is a simple structure based on the concept of a non-linear amplitude control of a voltage source inverter (VSI) output voltage. The validity of the proposed method will be demonstrated with the simulation results and the experimental results. Loss analyses are included in the paper to evaluate the efficiency of the two proposed methods. Furthermore, a 1 kW prototype was tested and efficiency of 93.5% is obtained.

Index Terms— Indirect Matrix Converter, PWM, AC/AC converter, Over modulation, Square wave, Trapezoidal wave

I. INTRODUCTION

The developments of energy saving converters are studied and researched intensively due to the global warming issue. Especially in the field of transportation, three phase converters are heavily used in motor drive applications, such as Hybrid Electric Vehicles (HEVs) or electric trains.

The Back to back converter which is composed by a voltage source rectifier and a voltage source inverter with an energy storage component at the DC link, is commonly applied in the industrial. However, the electrolytic capacitors are known with problems such as size and costing. Consequently, the direct type of AC/DC converters without the need of energy storage devices are actively studied, which can be classified into; conventional matrix converter (CMC) [1]-[4] and indirect matrix converter (IMC) [5]-[8]. These matrix converters deliver advantages in term of size and cost due to no energy storage components and also provide benefits such as high efficiency, unity power factor and energy regenerative.

However, the matrix converter faces a limitation in the output voltage transfer ratio at output voltage < 0.866 input voltage because of the output voltage is directly from the input voltage by merely controlling the switching devices with the applied modulation. When matrix converters are used in motor application, the motor capability will be degraded by approximately 15%. Further, under the same

output power condition with a back to back converter, the output current of the matrix converter will be higher than the back to back converters which will results the motor loss increased. Many researches have shown interests in term of improving the output voltage transfer ratio [9]-[11]. Similarly, IMC is having a same problem with the CMC, the limitation on the output voltage restricts the application of this converter. This paper will be discussing and analysis about the improvement on the voltage transfer ratio of an IMC.

This paper proposes two over modulation control methods aiming to improve the output voltage ratio of an indirect matrix converter. The proposed method does not need extra reactive components or switches to improve the output voltage transfer ratio. Since the indirect matrix converter can be divided into two stages; the secondary side which is similar to the voltage source inverter can be applied easily with a single pulse modulation (square-wave inverter). The modulation will transform the output voltage into a square wave from sinusoidal waveform (PWM) and improve the amplitude of the output voltage. The second proposed control is to transform the output voltage into a trapezoidal shape and so to increase the amplitude of the output voltage too [12].

Simulation results and experimental results will be demonstrated in the paper to show the validity of the proposed method. Furthermore, loss comparison between the simulation and experimental will be discussed in the later chapter as well.

II. CIRCUIT TOPOLOGY

Fig. 1 shows the circuit configuration of an indirect matrix converter. The indirect matrix converter can be divided into primary stage and secondary stage. The primary stage for the 3-phase input power source consists of six units of reverse blocking IGBT (RB-IGBT) also known as a current source rectifier. A LC filter is used at the primary side to smooth the input current. The secondary stage consists of six IGBTs is similar to a standard voltage source inverter that is connected to a load or motor. A snubber circuit is included at the DC link part of the converter for protection purpose. This snubber circuit will absorb overshoot voltage from the reactive elements in the circuit therefore only a small capacitance value is needed.

Among the many control modulation methods, two methods are well known for achieving high efficiency; the first is the zero current switching (ZCS) applying at the primary side [7]-[8]. The switches in the primary side can switch at zero switching loss when the secondary side is in zero vectors. During the zero vectors, the load current will be circulating inside the secondary side and the DC link current will be dropped to zero.

The second is known as the zero voltage switching (ZVS) that is applying at the secondary side [13]. For this control, two of the switches in the primary will turn on together to create a zero vector period and hence allow the IGBTs in the secondary side to switch without switching loss. During the zero vectors, the DC link voltage will drop to zero and the voltage is not formed in the secondary side and therefore loss can be reduced while switching.

However, in the over modulation methods, the secondary side will be driven with square wave or trapezoidal wave and zero vector periods are not occurring on both the primary side neither the secondary side. Therefore, efficiency is one of the concern factors which will be discussed in the later chapter.

III. OVER MODULATION CONTROL BLOCK DIAGRAM

Equation 1 shows that in the view of the secondary side, the input voltage could be considered as the DC link voltage (E_{dc}), and the DC link voltage is formed based on the 3-phase input voltage with the control in primary side as shown in (2), where S_{xy} stands for the switching units. When S_{xy} is turned on, $s_{xy} = 1$ and when S_{xy} is turned off, $s_{xy} = 0$. $[v_u \ v_v \ v_w]$ is the output voltage, $[E_{dcp} \ E_{dcn}]$ is the DC link voltage and $[v_r \ v_s \ v_t]$ is the input voltage.

$$\begin{bmatrix} v_u \\ v_v \\ v_w \end{bmatrix} = \begin{bmatrix} s_{up} & s_{un} \\ s_{vp} & s_{vn} \\ s_{wp} & s_{wn} \end{bmatrix} \begin{bmatrix} E_{dcp} \\ E_{dcn} \end{bmatrix}. \quad (1)$$

$$\begin{bmatrix} E_{dcp} \\ E_{dcn} \end{bmatrix} = \begin{bmatrix} s_{rp} & s_{sp} & s_{tp} \\ s_{rn} & s_{sn} & s_{tn} \end{bmatrix} \begin{bmatrix} v_r \\ v_s \\ v_t \end{bmatrix}. \quad (2)$$

Fig. 2 shows the proposed control block diagram originally from ref. [14]. The primary side controller is designed with a current type PWM rectifier command. The DC link voltage is formed from the maximum input phase voltage and the medium input phase voltage through the switching patterns of one phase modulation. Then, it uses a simple logic selector to convert the pulse pattern from the voltage source into a current source. The DC link voltage will contain a ripple with 6 times of the input frequency, where a 3-phase 200 V input voltage can deliver a sufficient DC link voltage at 270V.

The voltage source inverter is applied with a lean controlled carrier modulation to distribute the zero period of the DC link current. The lean carrier is controlled by the rectifier command (Rec_duty in primary side). Then, the zero current periods are allocated on the switching timing of the

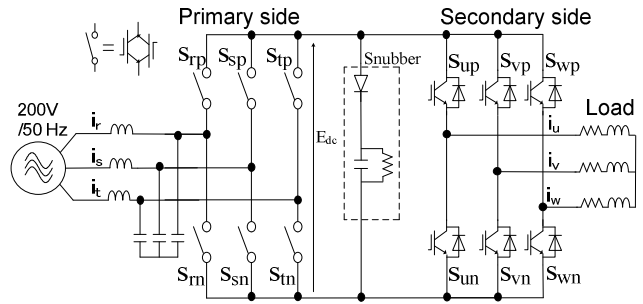


Fig.1. Circuit topology of an Indirect Matrix Converter (IMC).

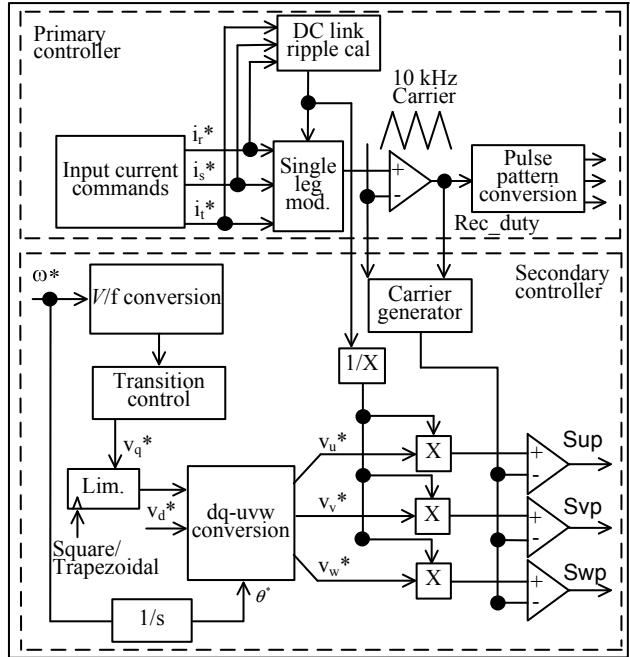


Fig.2. Proposed control block diagram.

primary switches. Therefore, the zero current switching (ZCS) is achieved on the primary side based on the rectifier command and the new carrier.

In the proposed method, no extra optimize control is required in the primary side control. On the other hand, the secondary side is added with a V/f conversion and transition control for the adjustable speed drive application in an induction motor. Practically, under the V/f constant condition, the maximum output voltage of the IMC is 173 V at output frequency 43 Hz due to the 0.866 limitation with a two phase modulation in the secondary side. In the proposed methods, the transition control is designed to start the transformation on the output voltage at 40 Hz and finished at 50 Hz. A sinusoidal waveform will rapidly change over to a square wave or a trapezoidal wave within the transition period.

The transition control is based on the non-linear control of the amplitude of the output voltage [15], which is a proportional compensation to the amplitude of output voltage command. The amplitude of the V_q^{*} will be expended in the over modulation range according to the frequency. Then, the output voltage command in three-phase will be calculated

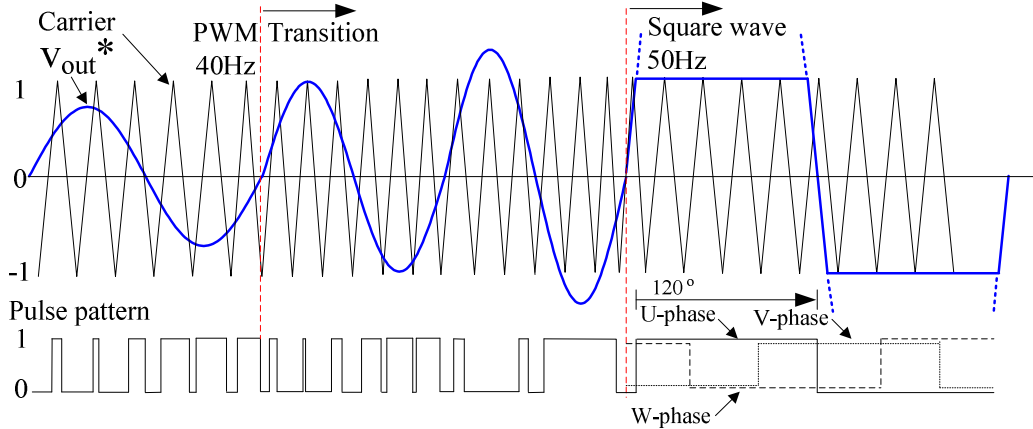


Fig. 3. Square wave modulation with transition control.

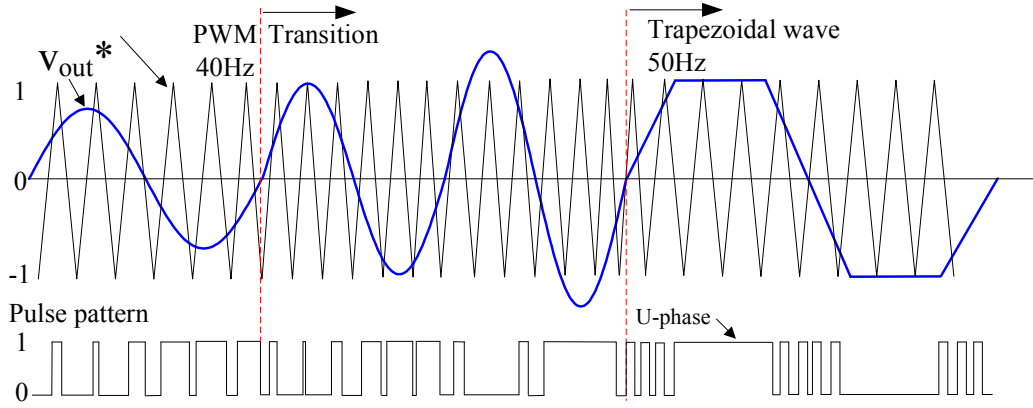


Fig. 4. Trapezoidal wave modulation with transition control.

from the dq conversion. A limiter is included before the dq conversion to switch between the two proposed control methods; which is the square wave and the trapezoidal.

A. Square wave modulation (Single pulse modulation)

Fig. 3 explains the operation of the Square wave modulation. The transition start from 40 Hz and the amplitude of the output voltage command is increasing according to the frequency. When the voltage command comes closed to the 50 Hz, the amplitude of the output voltage command is approximately 200 times larger than the PWM voltage command. Since the voltage command is always limited by the peak-peak of the carrier, therefore a nearly square wave will be formed. At the bottom of the Fig. 3 shows the pulse pattern in the secondary side. (The gate pulse will be active if the carrier is larger than the voltage command.) Once the transition is completed, each of the phases is switched at 120 degree phase angle, and zero vectors are not occurring. Furthermore, in the square wave modulation, the switching frequency is a lot lower than the PWM, and therefore the switching loss in the secondary stage is greatly been reduced.

B. Trapezoidal wave modulation

Trapezoidal wave modulation is another method that have been discussed and shown a possibility to increase the amplitude of the output voltage in the matrix converter [12]. The second control method is to propose using a trapezoidal wave modulation in the secondary side of the indirect matrix converter. Fig. 4 illustrates the transition control of the trapezoidal waveform. The control is basically the same as the square wave control. The transition control will start at 40 Hz and completed by 50 Hz. However, the extension of the V_q^* is being limited in the transition period in order to achieve a trapezoidal waveform with a rising angle of 40 degree. Although trapezoidal wave has more switching times than the square wave in one period cycle, the zero vectors are not occurring either.

The comparison and discussion between these two control methods will be discussed together with the simulation results in the next chapter.

IV. SIMULATION RESULTS

Since the zero vector periods are not occurring in the both control methods, the switching devices in the primary side requires a dead-time while switching. However, by applying

dead-time into the primary side, the dead-time period will cause a voltage distortion area in the DC link voltage. The dead-time period is considered as an open circuit in the primary side, and the DC link voltage will drop to zero. This is indirectly affecting the output voltage by referring to (1).

On the other hand, the hard switching in the primary side does not require a commutation with the secondary side. This is because of the switching pattern of the secondary side is at 120 degrees, therefore while the primary side is switching the secondary side will be in free wheeling mode as shown in Fig. 5. The output current will be circulating among the IGBTs and diodes even the primary side is at open circuit. In Fig. 5 S_{up} , S_{vn} and S_{wp} are remaining at ON while the switching units in the primary side are turning On/Off.

Table 1 shows the simulation parameters for both the control methods. All simulation results are simulated by circuit simulator (PSIM, Powersim Technologies Inc.).

A. Square wave modulation

Fig. 6 shows the simulation result by applying the square wave modulation with a transition control. The transition control is programmed to start at output frequency 40 Hz and completed by 50 Hz, which is referring to the Fig. 6, the over modulation starts at 0.8s and stop at approximately 1s. During the transition process, there is no surge voltage found in either the input side or the output side. The input current I_r is keeping a nearly sinusoidal waveform through out the process, and the output current I_u can keep a sinusoidal waveform and then transformed into a six-step waveform when the output voltage command becomes a square wave. Before the transition control begins (PWM), at 40 Hz, the input current I_r is 3.25 A, the output current I_u is 3.78 A and the output line-line voltage V_{uv} is about 170 V (RMS). After completing the transition, at 50Hz, the input current I_r is about 4.34 A, the output current I_u is 4.38 A that is nearly equal to the input current and the output line-line voltage V_{uv} is 198 V(RMS). Note that this is an ideal condition, dead time effect is not being considered.

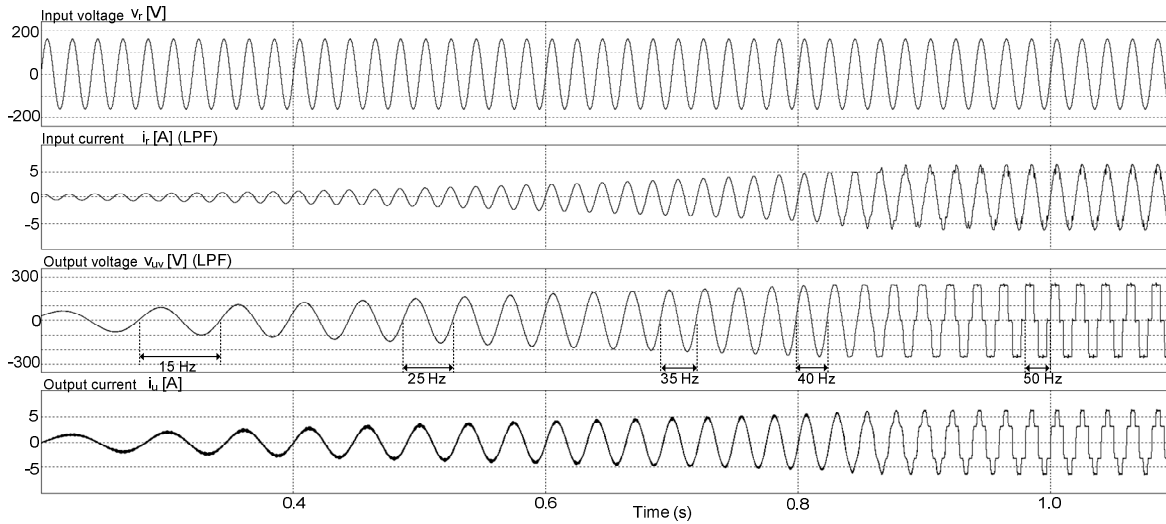


Fig.6 Simulation results (From PWM to square wave modulation)

Fig. 7 shows another simulation result with the square wave modulation. This result included the dead time in the switching units and the output frequency is 120 Hz. As previous discussed, the DC link voltage E_{dc} is found dropping to zero frequently during the dead time period. The output line-line voltage V_{uv} is 189 V(RMS), and the output voltage transfer ratio is 0.94.

Other than that, the input current cannot keep a sinusoidal waveform due to the six-step waveform in the output current. The input current is found distorted and the harmonic components are increased.

B. Trapezoidal wave modulation

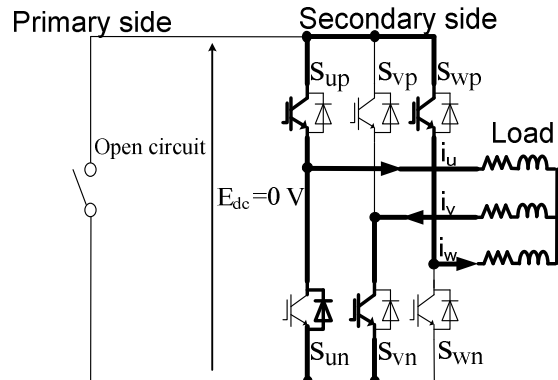


Fig. 5. Circulation of output current while primary side is open circuit.

TABLE I
SIMULATION PARAMETERS

Modulation	Square wave modulation	Trapezoidal wave modulation
Input frequency	50 Hz	50 Hz
Output frequency	50 Hz (Figs. 5, 13)	50 Hz (Figs. 9, 15)
Output frequency	120 Hz (Fig. 7)	50 Hz (Fig. 8)
Output power	1500 W	1500 W
Carrier frequency	10 kHz	10 kHz
Input voltage	200 V	200 V
Input power factor	98%	99%
Load condition	R = 25Ω, L = 1 mH	R = 25Ω, L = 5 mH

Fig. 9 demonstrates the simulation results by applying the trapezoidal wave modulation with the transition control. Note that this is an ideal condition, dead time effect is not included. The simulation conditions are the same as the Table 1. The transition starts at 40 Hz (0.8s in Fig.8) ends by 50 Hz (1s in Fig. 8). The simulation results show a smooth transformation process on the transition period. Both the input current and output current are in sinusoidal waveforms. At 40 Hz, the input current I_r is approximately 3.20 A, the output current I_u is 3.80 A and the output line-line voltage V_{uv} is approximately 168 V (RMS). After 50Hz, the input current I_r is 4.15 A, the output current I_u is 4.27 A and the output line-line voltage V_{uv} is 185 V(RMS).

Fig. 8 shows the simulation result with trapezoidal wave modulation that included the dead-time. Zero vector periods are not occurring in the secondary side and the DC link voltage E_{dc} will distorted due to the dead-time, same like the square wave modulation. The output line-line voltage V_{uv} is 178 V(RMS), and the output voltage transfer ratio is 0.89. However, the input current is found less distorted with the trapezoidal wave modulation. Further, the output current is in a sinusoidal waveform which means in the application of motor, the motor loss is lesser because the six-step waveform contains high harmonic components.

C. Comparison between the two proposed methods

Comparing between the square wave modulation and the trapezoidal modulation; in term of the voltage transfer ratio the square wave can achieve a better result. Furthermore, since the switching period for the secondary side is at 120 degrees, the switching loss is low and nearly to zero. However, the input current and the output current are containing high harmonic components.

The trapezoidal wave modulation is achieving a better result in term of harmonic components in the input current and the output current. However, the voltage transfer ratio is expected to be lower than the square wave modulation.

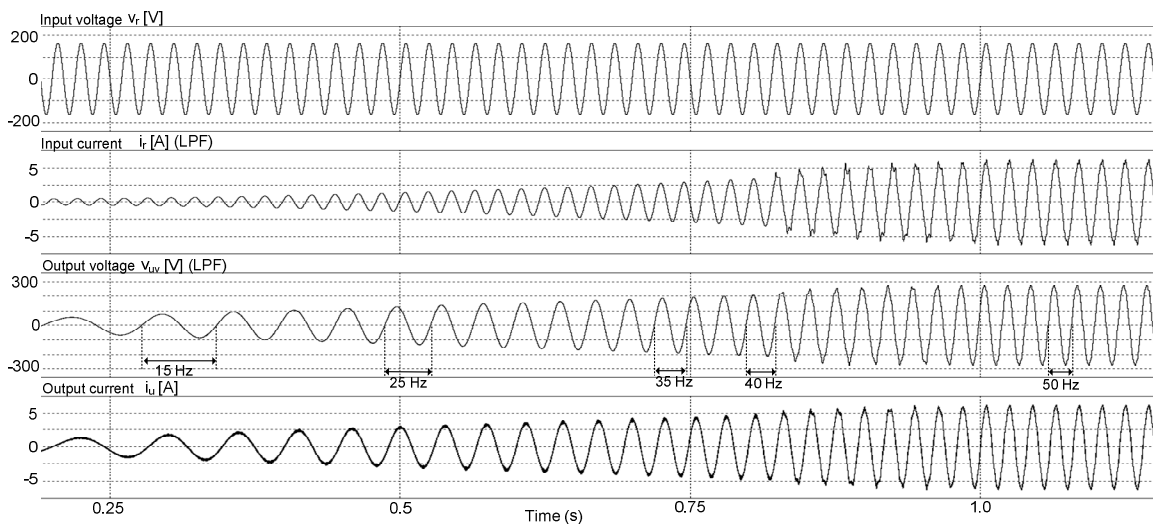


Fig. 9. Simulation results (From PWM to trapezoidal wave modulation)

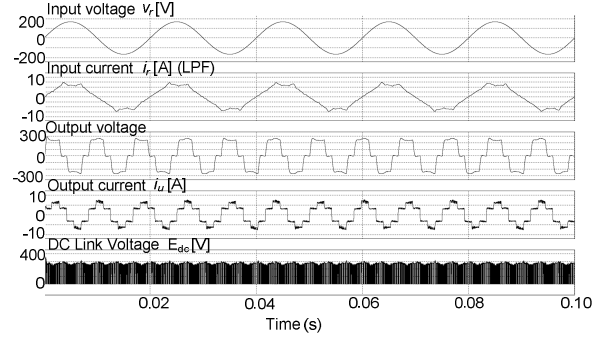


Fig. 7 Square wave operation simulation results.

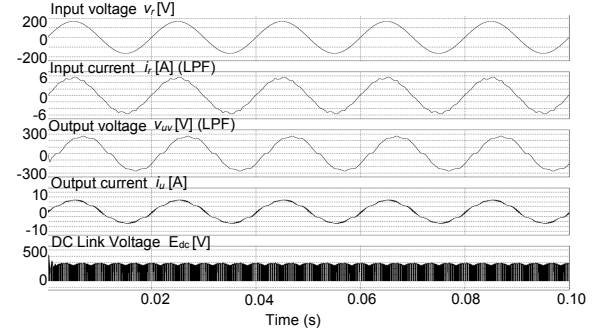


Fig.8 Trapezoidal wave operation simulation results.

V. EXPERIMENTAL RESULTS

Both the proposed methods were tested in a 1-kVA prototype and Table 2 shows the experimental parameters.

Fig. 10 shows the experimental results of the square wave operation. The input current I_r is 4.04 A, the output current I_u is 4.08 and the output line-line voltage V_{uv} is 183V. As discussed in the simulation section, the input current contains of distortion due to the six-step waveform in the output current. The voltage transfer ratio is improved from 0.866 to 0.92.

Fig. 11 shows experimental results of the trapezoidal wave operation. In this case, the input current I_r is 3.70 A, the

output current I_u is 3.91 A and the output line-line voltage V_{uv} is 175 V. The distortion in the input current is lesser and the output current is nearly to a sinusoidal waveform. The voltage transfer ratio is improved from 0.866 to 0.881.

Figs. 12(a) and 12(b) show the input current harmonic analysis between the square wave and the trapezoidal wave respectively. The input current THD of the square wave is 12.4 % and the input current THD of the trapezoidal wave is 9.7 %. Comparing between the Figs. 12(a) and 12(b), the input current of the trapezoidal waveform contains lesser high harmonic components than the square wave modulation. These results confirmed that the trapezoidal wave modulation can deliver a better THD input current and output current.

VI. LOSS ANALYSIS & EFFICIENCY

This chapter will be discussing the losses between the two proposed methods and then comparing the efficiency of these two methods between the simulation results and the experimental results. In other than that, the loss about the square wave modulation will additionally compare with another square wave modulation that comes with a zero current switching. The purpose of this comparison is to prove that under the single pulse modulation, even without the zero current switching, the converter still can remain high efficiency. Note that the switching devices in the primary side are assumed to be RB-IGBTs in the simulation analysis. The simulation condition does not consider about the dead time,

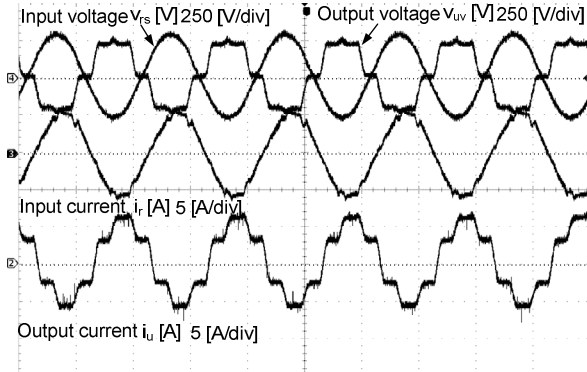


Fig. 10. Square wave operation experimental results.

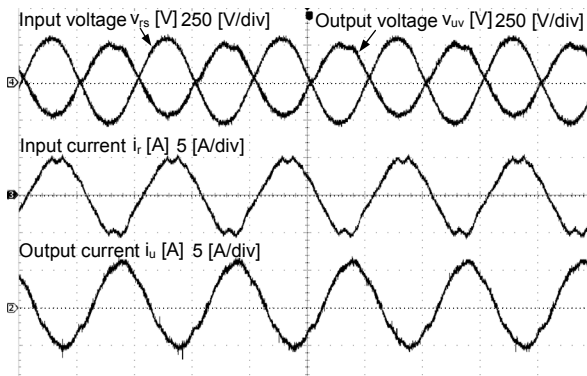


Fig. 11. Trapezoidal wave operation experimental results.

TABLE II
EXPERIMENTAL PARAMETERS

Modulation	Square wave modulation	Trapezoidal wave modulation
Input frequency	50 Hz	50 Hz
Output frequency	50 Hz	50 Hz
Output power	1500 W	1500 W
Input voltage	200 V	200 V
Output voltage	183 V	175 V

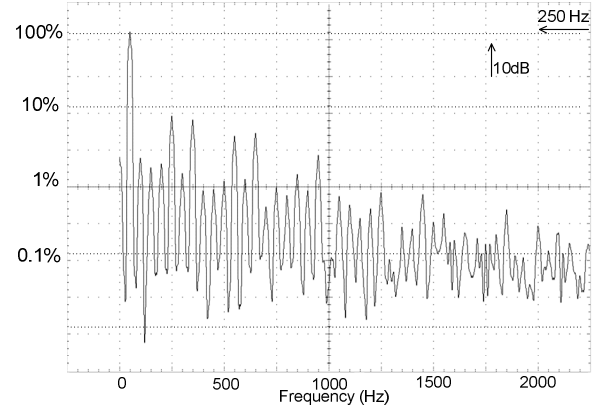


Fig. 12(a). Square wave modulation

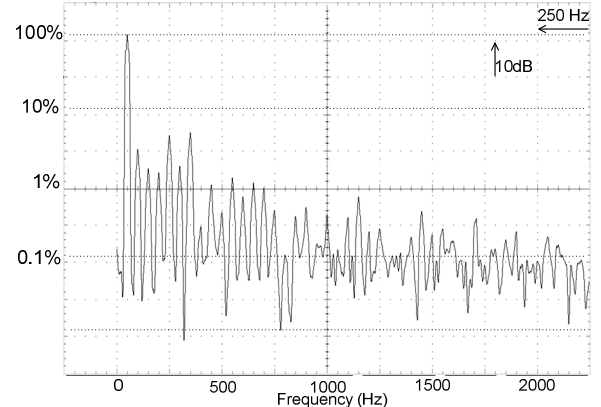


Fig. 12(b). Trapezoidal wave modulation
Fig. 12. Harmonic analysis of the input current.

LC filter loss and snubber loss. The simulation parameters are same as the Table 1 and the analysis method is from ref. [14].

A. Loss analysis – PWM and Square wave modulation

The proposed method can transform between the PWM and square wave easily and therefore an efficiency analysis between these two modulations is needed. Fig. 13 shows the loss comparison between PWM and square wave modulation. For the PWM, zero current switching can be applied in the primary side, and therefore the switching loss is zero. However, the PWM uses a 10 kHz carrier which results the switching loss is high in the secondary side. On the other hand, for the square wave modulation, the switching loss is moved from secondary side into the primary side. This is because the switching in the secondary side only happens at 120 degrees for each phase following the square wave operation, since the switching frequency is very low, the switching loss could be reduced nearly to zero. Further, the

frequency of the carrier is not affecting the switching loss of the secondary side. Also, the zero current switching cannot be applied and results that the RB-IGBT is containing switching loss.

In PWM, the loss for primary side is approximately 1.3 % and for secondary side is approximately 1.8 %. As for the square wave modulation, the loss in primary side is proximately 1.9 % and the secondary side is 1.1 %. From the results, we can understand the losses between the PWM and square wave are about the same.

B. Loss analysis –Square wave modulation (With & without zero current switching (ZCS))

This section will be discussed on applying a zero current switching (ZCS) into the square wave modulation. A limiter is included to the peak value of the square wave voltage reference, and force the peak value decrease from 1.0 (peak) to 0.95. Fig. 14 shows the diagram explanation of the spoken method. By this control, zero vector periods are occurring mostly at the peak of the carrier. The primary side can utilize these periods to achieve the zero current switching. However, this method will be affecting the amplitude of the output voltage where the voltage transfer ratio will be getting lower. The purpose of this comparison is to prove that the losses of these two modulations are about the same, even the zero current switching cannot be applied in the primary side.

Fig. 15 shows the loss comparison between the square wave modulations with and without the ZCS. For the square wave with ZCS, the loss in the primary side is approximately 1.9%, and the secondary side is eminently 1.1%, where the total losses are nearly the same to the square wave without ZCS; 28 W for a 1 kW system. From this analysis, we can understand that the proposed method can achieve high efficiency because of the square wave in secondary side which produce a low switching loss can replace the applying of ZCS in the primary side.

C. Loss analysis –Square wave modulation and trapezoidal modulation

The loss comparison between the square wave and trapezoidal is shown in Fig. 16. Note that the voltage and current of each modulation are different from each other although the power is same. For the square wave modulation, the input current I_i is 3.14 A, the output current I_u is 3.00 A and the output phase voltage V_u is 120 V. And for the trapezoidal, the input current I_i is 2.95 A, the output current I_u is 3.00 A and the output phase voltage V_u is 114 V.

The total loss for square wave is 28.65 W and the trapezoidal is 28.58W. The analysis shows that these two modulations have a similar loss under a same output power. Therefore, both the modulations are capable to achieve high efficiency at around 97%. Note that if all switching units in the primary side are formed by the series connected of two IGBTs, the efficiency is approximately decreased by 2% due to the existing of diode conduction loss (FWD).

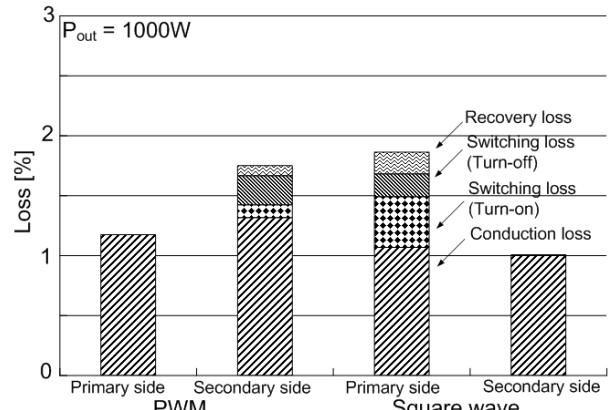


Fig. 13. Loss comparison between PWM and square wave.

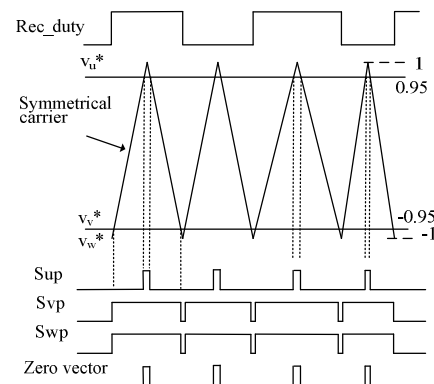


Fig. 14. Explanation of square wave modulation with zero vectors.

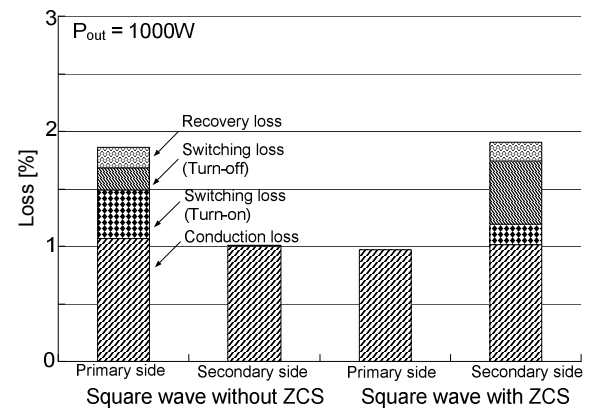


Fig. 15. Loss comparison between square wave with ZCS and without ZCS

D. Experimental Efficiency

The last chapter will be covering the efficiency of the two proposed methods. The parameters are the same as the experimental section in chapter V. Note that the switching units in the primary side is a series connection of two IGBTs in one unit. First the efficiency for the square wave modulation that includes the transition from PWM to square wave is demonstrated in Fig. 17. The output frequency ratio is shown at the bottom where 1= 50 Hz and so on. In the graph, below than 0.8 is the PWM operation and the square wave starts at 1.0. It can be known that the efficiency is

keeping constantly at around 93.5 % even the transition is involved under various power.

Fig. 18 shows the efficiency comparison among the square wave modulation, trapezoidal modulation and simulation analysis of square wave modulation. The assumed filter losses are including the LC filter in the primary side and the snubber circuit at the DC link part. Experimental efficiency shows 93.5 % for the two proposed methods and simulation analysis shows 94 % for square wave modulation.

VII. CONCLUSION

This paper proposed two over modulation methods that aim to improve the output-input voltage transfer ratio of an indirect matrix converter. The two proposed methods are demonstrated in simulation and experimental results. These results and analysis have proven the validity of the proposed methods. The voltage transfer ratio is 0.92 for the square wave modulation and 0.88 for the trapezoidal wave modulation. Further, both modulations can achieve efficiency up to 93.5 % averagely by using series connected IGBTs in the primary side.

REFERENCES

- [1] Sahoo, A.K.; Meenakshi, J.; Dash, S.S.; and Thyagarajan, T. "Analysis and simulation of matrix converter using PSIM", in *7th international conference on ICPE Power Electronics*, Daegu, pp. 414-419, Oct. 2007.
- [2] Lixiang Wei; Lukaszewski, R.A and Lipo, T.A. "Analysis of Power-Cycling Capability of IGBT Modules in a Conventional Matrix Converter", *IEEE Trans. on Industry Applications*, Vol. 45, Issue. 4, pp. 1443-1451, Aug. 2009
- [3] Jun-ichi Itoh, Sato, I., Odaka, A., Ohguchi, H., Kodachi, H., and Eguchi, N, "A Novel Approach to Practical Matrix Converter Motor Drive System with Reverse Blocking IGBT", *IEEE Trans. Power Electronics*, Vol 20, pp. 1356-1363, Nov. 2005
- [4] Klumpner, C.; Blaajerg, F; Boldea, I.; and Nielsen, P. "New modulation method for matrix converters", *IEEE Trans. on Industry Applications*, Vol. 42, Issue. 3, pp. 797-806, June 2006.
- [5] Friedli, T.; Round, S.D.; and Kolar, J.W. "A 100 kHz SiC Sparse Matrix Converter", in *IEEE Power Electronics Specialists Conf.*, Orlando, pp. 2148-2154, June 2007
- [6] Gang Li; Kai Sun; and Lipei Huang, and Seiki Igarashi "RB-IGBT gate drive circuit and its application in two-stage matrix converter", in *23rd Annual APEC*, Austin, pp. 245-251, Feb. 2008
- [7] Kolar, J.W.; Schafmeister, F.; Round, S.D.; and Erthl, H. "Novel Three-Phase AC-AC Sparse Matrix Converters", *IEEE Trans. Power Electronics*, Vol. 22, Issue. 5, pp.1649-1661, Sept. 2007
- [8] Kato, K.; and Itoh, J.-i. "Control method for a three-port interface converter using an indirect matrix converter with an active snubber circuit", in *13th Power Electronics and Motion Control Conference*, Poznan, pp. 581-588, Sept. 2008.
- [9] Thuta, S.; Mohapatra, K.K; and Mohan, N. "Matrix converter over-modulation using carrier-based control: Maximizing the voltage transfer ratio", in *IEEE Power Electronics Specialists Conf.*, Rhodes, pp. 1727-1733, June 2008.
- [10] Satisch, T.; Mohapatra, KK; and Mohan, N. "Steady State Over-Modulation of Matrix Converter Using Simplified Carrier Based Control", in *33rd Annual Conference Industrial Electronics Society*, Taipei, pp. 1817-1822, Nov. 2007.
- [11] Itoh, J.-i.; and Maki, K. "Novel control strategy for synchronous PWM on a Matrix Converter", in *IEEE Energy Conversion Congress and Exposition*, San Jose, pp. 3049-3056, Sept. 2009.
- [12] Tamai, Y.; Ohguchi, H.; Sato, I.; Odaka, A.; Mine, H.; and Itoh, J.-i. "A Novel Control Strategy for Matrix Converters in Over-modulation

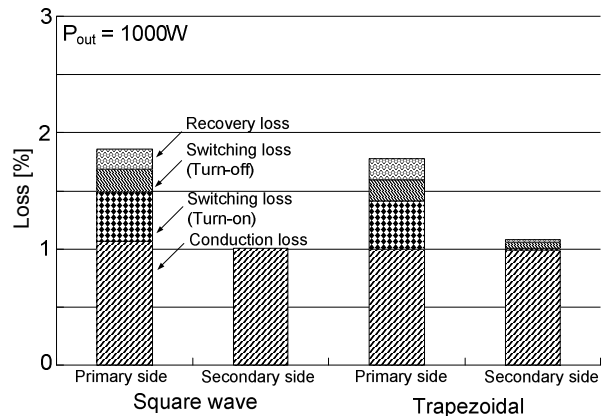


Fig. 16. Loss comparison between square wave and trapezoidal wave.

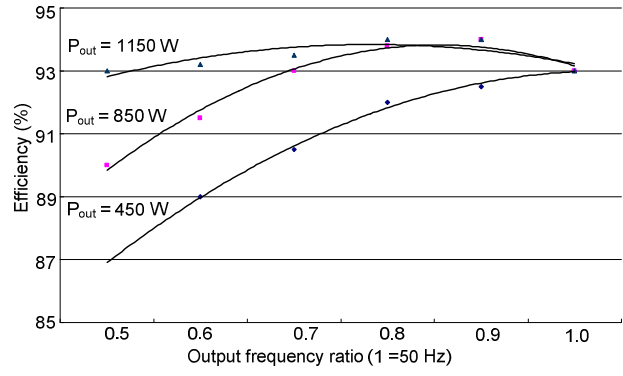


Fig. 17. Experimental efficiency of square wave with transition control.

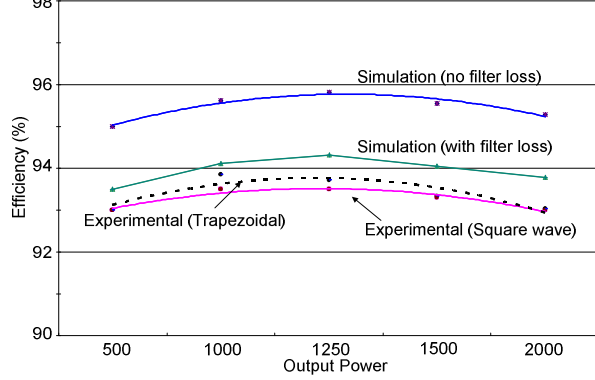


Fig. 18. Comparison of efficiency.

- Range", in *Power Conversion Conference*, Nagoya, pp. 1049-1055, April 2007.
- [13] Itoh, J.-i.; Hinata, T.; Kato, K.; and Ichimura, D. "A novel control method to reduce an inverter stage loss in an indirect matrix converter", in *35th Annual Conference Industrial Electronics*, Porto, pp. 4475-4480, Nov. 2009
 - [14] Goh Teck Chiang; and Itoh, J.-i. "A three-port interface converter by using an indirect matrix converter with the neutral point of the motor", in *IEEE Energy Conversion Congress and Exposition*, San Jose, pp. 3282-3289, Sept. 2009.
 - [15] Itoh, J.-i.; and Ohtani, N. "Square wave operation for a single-phase PFC three-phase motor drive system without a reactor", in *International Conference ICEMS*, Tokyo, pp. 1-2, Nov. 2009.